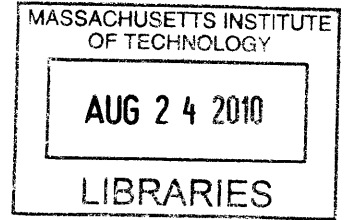


Fast Scanning Two-Photon Microscopy

by

Jeremy T Chang

[S.B. EE, M.I.T., 2009]



Submitted to the Department of Electrical Engineering and Computer Science

in Partial Fulfillment of the Requirements for the Degree of

Master of Engineering in Electrical Engineering and Computer Science

at the Massachusetts Institute of Technology

ARCHIVES

May, 2010

[June 2010]

©2010 Massachusetts Institute of Technology

All rights reserved.

Author _____
Department of Electrical Engineering and Computer Science
May 21, 2010

Certified by _____
Dr. Edward S Boyden
M.I.T. Thesis Supervisor

Accepted by _____
Christopher J. Terman
Chairman, Department Committee on Graduate Theses

Fast Scanning Two-Photon Microscopy

by

Jeremy T Chang

Submitted to the
Department of Electrical Engineering and Computer Science

May 21, 2010

In Partial Fulfillment of the Requirements for the Degree of
Master of Engineering in Electrical Engineering and Computer Science

ABSTRACT

Fast scanning two-photon microscopy coupled with the use light activated ion channels provides the basis for fast imaging and stimulation in the characterization of in vivo neural networks. A two-photon microscope capable of fast scanning using acousto-optic deflectors was designed and implemented. The software controller was expanded so that random access scan in three dimensions could be handled, so that algorithms that can identify neurons from images acquired using the two-photon microscope can be developed. Finally the localization of optogenetic Channelrhodopsin-2 channel to the neuron cell body was tested using a Chr2-MBD construct.

Thesis Supervisor: Edward Boyden

Title: Benesse Career Development Professor, MIT Media Lab

Acknowledgement

I'd like to thank by advisor Ed Boyden for all his guidance through the duration of this thesis, Amy Chuong, Brian Chow and the rest of the Synthetic Neurobiology group for all the insights and help with the training for confocal microscopy, preparing the MBD construct, culture preparation, and general insights. Also Neil Gershenfeld and the Center for Bits and Atoms for the use of the space and femtosecond laser. Lastly I'd like to thank my parent and friends for all the encouragement and support they've given me in seeking to achieve my dreams.

Table of Contents

ABSTRACT.....	2
List of Figures	5
1. Introduction.....	6
1.1. Organization of Thesis	8
2. Problem	9
3. Background.....	11
3.1. Confocal Microscopy.....	11
3.2. Two-Photon Microscopy.....	12
3.3. Two-Photon Microscope Design Considerations.....	15
3.4. Fast Scanning Using Acousto-Optic Deflectors	16
4. Two-Photon Microscope Construction and Specifications	19
4.1. Specifications	19
4.2. Neurospy Software	24
4.3. Imaging.....	27
5. Two-Photon Activation of Targeted ChR2.....	33
5.1. Localization of ChR2.....	33
5.2. Two-Photon Activation and Saturation of ChR2.....	37
5.3. Scanning ChR2.....	39
6. Further Work	42
7. Conclusions.....	44
8. References.....	45

List of Figures

Figure 1: Two-Photon Absorption Jablonski Diagram.....	13
Figure 2: Comparison of Confocal and Two-Photon Microscope Setup.....	14
Figure 3: Cylindrical Lens Using Acousto-Optic Deflectors	17
Figure 4: Laser Spectrum.	20
Figure 5: Kapteyn-Murnane Labs Ti:Sa Laser.....	21
Figure 6: Block Schematic of Two-Photon Setup.	23
Figure 7: Sample of Random Access Waveform in Two Dimensions.....	25
Figure 8: Sample of Chirped Waveform in Three Dimension.	26
Figure 9: Schematic of Fluorescent Well.	27
Figure 10: Images of Polystyrene Microsphere.	28
Figure 11: Image and Analysis of Noise.	29
Figure 12: Pattern of Illumination.....	31
Figure 13: Expression of Chr2-MBD	35
Figure 14: Chr2 expression.....	36
Figure 15: Two-Photon Activation of Chr2.....	39
Figure 16: Generated Scan Pattern.....	41

1. Introduction

In order to bridge the gap between synaptic activity and higher level functions in the brain, it is necessary to have tools that can track changes over time in the strength of synaptic connections of neural circuits. Tools that can probe the brain at this level could further extend our understanding of the basis of disorders such as Alzheimer's Disease, Parkinson's Disease, epilepsy, brain trauma, and post-traumatic stress disorder. Understanding the neural basis of these disorders could further inform diagnosis and treatment allowing for specifically targeted methodologies.

Of particular interest are changes that occur in synaptic connections and strength over time. Preserving the structure of the brain is necessary in order to be able to probe the brain over the course of time, therefore the modality used to map neural circuits must be preserve the tissue of the brain. Traditionally electrodes have been used to stimulate and record from the brain. Inserting an electrode into the brain has many downsides including lack of specificity and destruction of brain tissue.

Methods that utilize light to probe into deep tissue could allow the testing of neural circuits with minimal physical damage to tissue. Channelrhodopsin-2 (ChR2) and other optogenetic controls have proven to be useful tools for the optical modulation of neural circuits using single-photon excitation [1-3]. Many of these optogenetic controls are light gated ion pumps or channels expressed with the cell membrane, used to drive currents within neurons to modulate electrical activity.

Single photon activation of these proteins limits the region of the brain which can be studied without causing physical damage by inserting fiber optics. Using high powers of light without a fiber optic to get to deeper structures has the downside of higher probability phototoxicity and nonspecific

activation of neuron. Two-photon absorption in fluorophores has been employed in microscopy in order to increase the depth of imaging in tissue, and can be leveraged to localize the activation of optogenetic proteins increasing the depth of region available to study within the brain without insertion of a fiber into the brain, minimizing physical damage to brain tissue.

In order to be able to target individual neurons for stimulation, it is necessary to image and identify neurons. The advantages of two-photon absorption can be leveraged here as well. The laser beam used to stimulate a neuron can also be used to image the area of interest, through two-photon microscopy. Unlike traditional confocal microscopy, two-photon microscopy can image into deep tissue, allowing the brain to be kept intact.

Since the rate of two-photon absorption scales with the square of the intensity of the light incident on the fluorophore the probability of absorption outside of the focal volume is very low, localizing the absorption and emission [4]. The longer wavelength photons are also less likely to scatter in tissue, and the lower power of each photon is less likely to cause photobleaching and phototoxicity which increases the depth in tissue at which imaging and stimulation could occur.

Two-photon activation of ChR2 has been difficult, however, due to the limited current that can be delivered to the neuron. By scanning efficiently across the membrane of the neuron, a sufficient current can be produced in order to spur action potentials. Previous attempts to drive ChR2 with two-photon activation have shown the limitations that arise due to the long activation of ChR2 and the localized nature of two-photon activation [5, 6]. The purpose of this project is to construct a two-photon microscope using acousto-optic steering in three dimensions, to demonstrate that action potentials within a neuron can be achieved through fast scanning.

1.1. Organization of Thesis

This thesis discusses the design and implementation of a functional two-photon microscope using acousto-optics for scanning in three dimensions. Section two will outline the problem being solved. Section three will give an overview of the prior work done in Two-photon microscopy and two-photon activation of ChR2. Section four and five will present the solutions in detail addressed by the thesis. Section six proposes the next steps that could be taken. Section seven will provide final remarks and conclusions for the thesis.

2. Problem

The goal of this thesis is to lay the framework in which neural circuits can be mapped in live intact animals. The thesis addresses three technologies that needed to be developed in order to move toward in vivo stimulation and recording of neural circuits. The first is to build a two-photon microscope capable of fast scanning. The second is to develop software that can identify neurons from images acquired using the two-photon microscope. The final concerns localization of the optogenetic channelrhodopsin-2 channel at the neuron cell body.

The first stage of this thesis is to build a custom two-photon microscope that uses acousto-optics for fast scanning. Building a microscope from the ground up presents many challenges, including assembling parts and writing custom software. The benefit of building a two-photon microscope, however, is that the overall system ends up being lower cost and readily customizable. The microscope built employs acousto-optic deflectors for beam steering which will allow for fast scanning across a sample.

The second stage of the thesis is to build scan patterns that are capable of scanning neurons at fast speeds in three dimensional space in order to stimulate neurons quickly. Using segmentation algorithms and automated recognition of neurons provides consistent results in stimulation, and can quickly find the most efficient scan patterns. The added benefit of the speed of analysis is also useful when dealing with living tissue such as brain slices or live animals, that have a limited useful lifetime before tissue death begins to occur.

The final portion of this thesis explains and demonstrates the localization of ChR2 to the somatodendritic portion of the neuron. Localizing the expression of ChR2 in the soma of neurons is essential in order to minimize the chances of co-localized axons from being stimulated. These axons could extend from regions of the brain that are not of interest, and could make it difficult to analyze the neural circuit of interest.

3. Background

Optical methods of observation of structures within the brain, offer many advantages over other imaging methodologies such as MRI such as imaging at the cellular and sub cellular level as well as targeted selectivity of neurons observed. Coupled with patch-clamped electrode recording, stimulated activity in the brain can be monitored at the synaptic level where as fMRI tracks the activity of larger regions of the brain through changes in blood flow. Imaging methods, however, have limited the use of patch-clamping to cultures and slices. This section will outline some of the drawbacks of traditional confocal microscopy, basis for two-photon microscopy, design considerations for two-photon microscope, and basis for fast scanning using acousto-optic deflectors.

3.1. Confocal Microscopy

Confocal microscope imaging of fluorescent neurons has been a common method for observing structures within neuron cultures and brain slices. By using a pinhole detector, photons that are scattered or generated from outside the focal plane are discarded. These scattered and out of plane photons increase the noise of images and limit imaging depth in traditional epifluorescence microscopy.

Confocal microscopy, however, wastes useful excitation since absorption occurs in a broad area surrounding the focal volume and only photons from a small region in the focal plane are used to reconstruct the image. In addition, scattering of fluorescence lowers the available useful signal necessitating higher excitation energies. This means that the rate of photobleaching of fluorophores per image is higher than necessary.

3.2. Two-Photon Microscopy

Using the absorption of two photons in a single fluorophore, Denk et al. constructed a two-photon laser scanning microscope which mediated the problems that arise with confocal microscopy [7, 8]. While the probability of single-photon absorption scales linearly with the spatial density of photons, two-photon absorption has a square dependence [4]. The lower probability of absorption and lower energy photons allow for imaging in deep tissue which are beyond the range of confocal microscopes.

In single photon absorption and fluorescence, a single photon is used to promote a molecule to an excited state, where it undergoes heat loss, then fluorescence. In two-photon absorption and fluorescence two photons of approximately half the energy of the single photon that are coincident on a molecule promote the molecule to an excited state. From the excited state the molecules once again relaxes giving off heat, then fluorescence. A Jablonski diagram of the mechanism behind single and two-photon absorption and fluorescence can be found in Figure 1.

The longer wavelength photons used in two-photon absorption have many benefits. They are less likely to scatter, and their lower energies are less likely to cause unnecessary photobleaching of fluorophores.

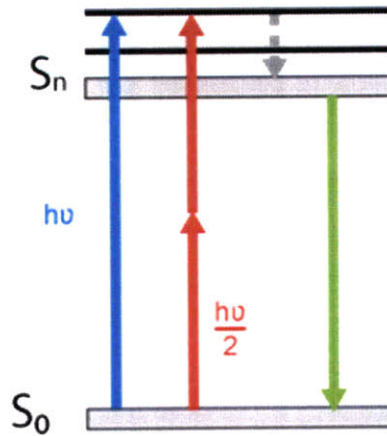


Figure 1: Two-Photon Absorption Jablonski Diagram. In single-photon fluorescence a single photon promotes the molecule to a higher energy state, which then relaxes through internal losses (heat) to a lower energy state, and then back to the ground state emitting a photon. In Two-photon absorption and fluorescence two photons of approximately half the energy are coincident on the molecule promoting it to the excited state.

The major drawback, however, is that the dependence on the square intensity of the laser necessitates the use of a pulsed laser in order to deliver a high density of photons to the focal volume. So et al, give the number of photons absorbed per fluorophore per pulse, for a pulsed laser excitation of a fluorophore where τ_p is the pulse duration as

$$n_a \approx \frac{p_0^2 \delta}{\tau_p f_p^2} \left(\frac{(NA)^2}{2\hbar c \lambda} \right) \quad (3.2.1.)$$

where δ is the two-photon absorption at excitation wavelength λ , p_0^2 is the square of the average laser intensity, f_p is the repetition rate, \hbar is Planck's constant, and c is the speed of light [9]. Equation (3.2.1.) underscores the advantage of using high NA objectives, as the absorption scales with the square of the NA.

Since the probability of absorbing two photons is much lower than a single-photon absorption at half the wavelength, two-photon absorption is restricted to the focal volume allowing all fluorescence generated, scattered or not, to be used as signal.

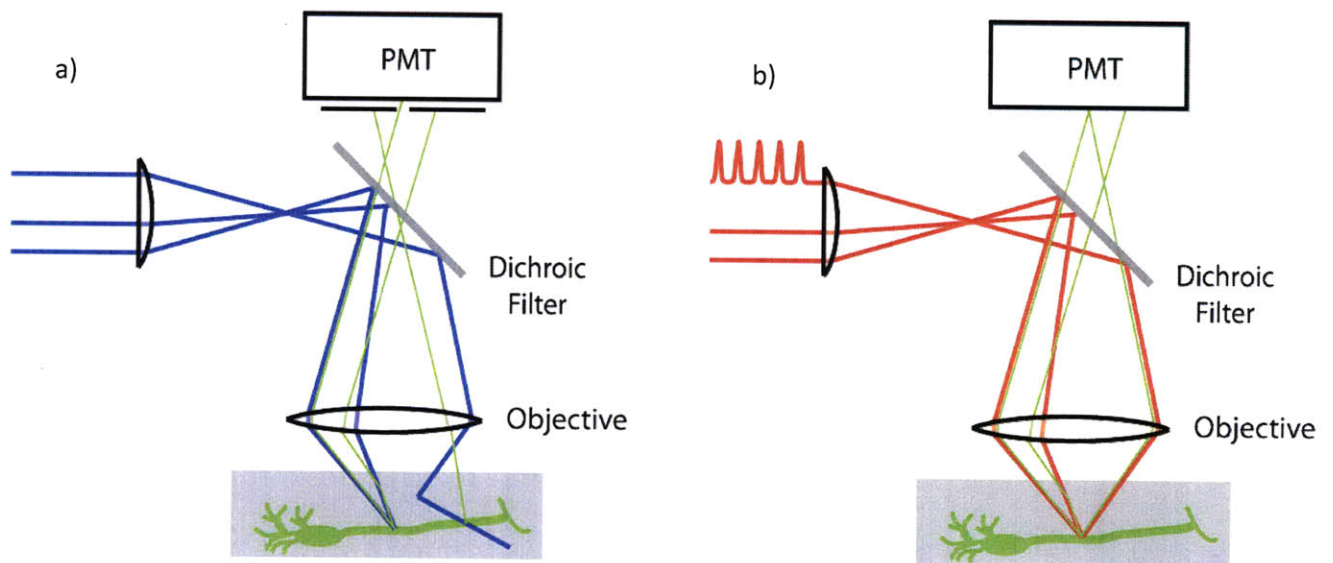


Figure 2: Comparison of Confocal and Two-Photon Microscope Setup. a) In a Confocal microscope a pinhole is used to discard fluorescence from outside of the focal volume. This pinhole also discards scattered fluorescence from the focal volume. b) Since fluorescence is only generated from the focal volume in two-photon microscopy, the pinhole can be discarded and all fluorescence can be used as signal. The laser, however, must be pulsed so that a high enough density of photons are present in the focal volume for two-photon absorption to occur.

To construct an image, a scanner is used to scan across the field of view. Traditionally these scanners have been x-y mirrors driven by galvanometers. Fluorescence photons are captured by a photosensor, which converts the fluorescence into a current signal. Photosensors that have been used include photomultiplier tubes (PMTs), avalanche photodiodes, and charge coupled device (CCD) cameras. When PMTs or avalanche photodiodes are used, software must take the signal and divide it into time bins, corresponding to pixels in the image. From this signal the image is reconstructed based on the known scan pattern.

3.3. Two-Photon Microscope Design Considerations

The resolution of the microscope can be measured in the axial as well as the lateral directions.

Tsai et al. define the worst case estimate of the axial resolution as

$$\delta z = 2 \frac{\lambda_0}{n} \left(\frac{n}{NA} \right)^2, \quad (3.3.1.)$$

where λ_0/n is the wavelength of in the tissue [4]. In this worst case estimate the intensity goes through the first zero along the optical axis. In the lateral direction, Tsai et al. show the worst case occurs when the first zero occurs along the radius in the focal plane. In this case the lateral resolution is given by the equation

$$\delta r = 0.6 \frac{\lambda_0}{n} \left(\frac{n}{NA} \right). \quad (3.3.2.)$$

The actual resolution of the microscope will depend on the fill of the back aperture of the objective [4]. While slightly overfilling the back aperture of the objective increases the resolution, underfilling the objective increase the power throughput. This is a tradeoff in the design of the optical pathway that must be considered.

The depth of imaging is dependent on a number of factors, including laser power, optical geometry, and tissue density. Two-photon microscopy has typically achieved imaging depths of <500 μm in brain. Lower magnification and higher NA objectives can extend this imaging depth by as much as 100 μm [10]. Other approaches have been used to further the depth of imaging. Gradient index (GRIN)

lenses have been reported to depths of $\sim 800 \mu\text{m}$ [11]. GRIN lenses, however, require that a needle like lens be inserted into the tissue of the brain. Using higher intensities of laser light can also increase imaging depth, but has diminishing returns causing lower contrast due to out of focus fluorescence [12].

Infinity-corrected objectives require that the incoming light must be collimated, thus a scan lens must be used. A tube lens also must be used in order to collimate any fluorescence light so that it can be viewed in an eyepiece. Together the scan lens and tube lens form a beam expander which can be used to overfill the objective. The scan lens and tube lens are typically parts of a modified epifluorescence microscope. The size of the field of view is thus limited by the size of the scan and lens tube and the scanning range. In the microscope built in this thesis, these considerations were not weighed as an epifluorescence pathway and eye piece were not employed. Field of view, therefore was only limited by the back aperture of the objective and the bandwidth of the AODs. See Section 4.1 for more details.

3.4. Fast Scanning Using Acousto-Optic Deflectors

The use of acousto-optic deflectors (AODs) has provided a basis for fast two-dimensional scanning in two-photon microscopy, allowing fast access to points in a single plane. Traditionally these microscopes require a mechanical method for focusing in the z-axis. However, by supplying a chirped wave (a sweep in frequencies) through two AODs an effective spherical lens can be made which allows access to individual points in three dimensions, eliminating the need for slow mechanical mechanisms for focusing. Controlling scanning in all three dimensions with AODs allows for scan rates higher than those of traditional galvanometer based steering methods.

The concept of using AODs to scan in three-dimensions was demonstrated by Reddy and Saggau who found that two AODs driven by chirped frequencies can have a tunable cylindrical focus [13]. Two

TeO₂ AODs were used to deflect a continuous wave argon laser ($\lambda=488\text{nm}$). The beam was then imaged onto a movable digital camera in order to find the effective focal length of the two AOD sub-system. Cascading two such subsystems orthogonally would then allow for static spherical focusing. One can use two orthogonal AODs to obtain a focus as well, however this places limits on scanning as the focal point is constantly moving, due to the chirping of the input acoustic signal.

The deflection of an acousto-optic deflector is given by Reddy and Saggau with the equation:

$$\theta = \frac{\lambda}{\Lambda} = \frac{\lambda f}{v}, \quad (3.4.1.)$$

where θ is the angle of deflection, λ the wavelength of the laser light, v the speed of sound in the crystal, f the acoustic frequency and Λ the wavelength of the acoustic wave in the crystal.

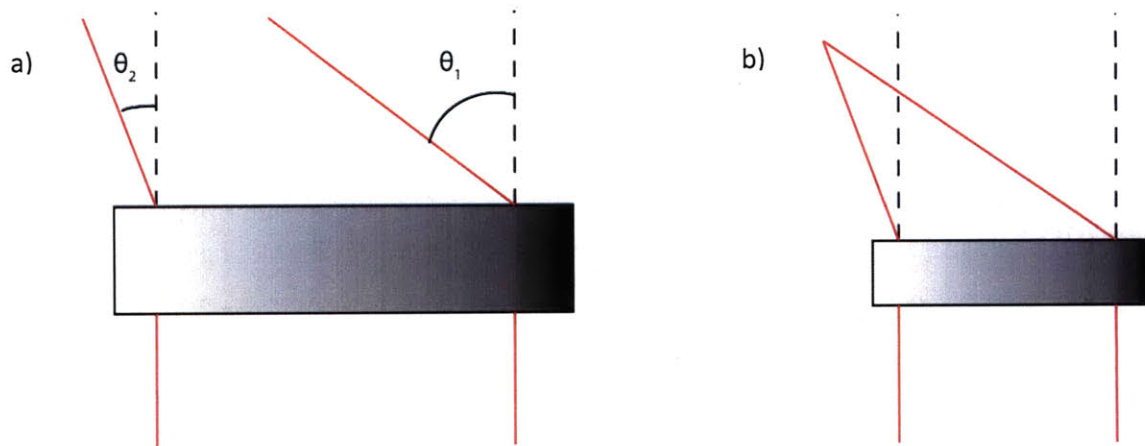


Figure 3: Cylindrical Lens Using Acousto-Optic Deflectors a) The deflection angle across the face of the beam increases as the fringe spacing in the crystal decreases. b) Deflection in angle across the face of the beam causes a cylindrical focus. Effects are shown exaggerated to emphasize effect and the zero order beam has been omitted for clarity.

By delivering a sweep in frequencies to an AOD an effective cylindrical lens can be made as seen in Figure 3. Substituting for f such that $f(t) = f_{min} + \alpha t$ (a linear sweep in frequencies) such that $\alpha = \Delta f / T_{scan}$ and T_{scan} is the duration of the chirp, θ becomes $\theta(x, t)$ a function of space a time defined by the equation Reddy and Saggau derived:

$$\theta(x, t) = \frac{\lambda}{v} (f_{min} + \alpha t) - \frac{\lambda \alpha}{v^2} x. \quad (3.4.2.)$$

An effective spherical lens can be made, if two telecentrically relayed AODs are driven by acoustic frequencies such that $f_1(t)$ is the acoustic signal to the first AOD, and $f_2(t)$ is the acoustic signal to the second AOD and $f_1(t) = f_2(t) = f_{min} + \alpha t$. Reddy and Saggau showed that the focal length for this effective lens is given by the equation

$$F_{AOD} = \frac{v^2}{2\lambda\alpha} = \frac{v^2 T_{scan}}{2\lambda\Delta f}. \quad (3.4.3.)$$

Thus by selectively choosing α and f_{min} the AODs can be used to scan in three dimensions[13]. While a focus can be achieved using chirped frequencies, the nature of the chirping causes the focus of the AODs to constantly move. There are two possible methods for coping with the non static nature of the focal point. The first is to couple four AODs in order to achieve true 3D random access to points [14]. In this approach the apertures of the AODs can limit the field of view. The second approach is to deal with the moving focal point by writing scan patterns that can appropriately compensate. The second approach is the one examined in the rest of this thesis.

4. Two-Photon Microscope Construction and Specifications

A custom built two-photon microscope was built employing AODs for beam steering in three dimensions. It was necessary to build a custom microscope so that a fast enough scan rate could be achieved for neuron stimulation. This section will outline the construction of a custom two-photon microscope, theoretical and practical limitations of the microscope, and development of scan patterns in the Neurospy software suite, and basic imaging.

4.1. Specifications

Excitation in the custom two-photon microscope is driven by a mode-locked KM Labs Ti:Sa laser centered at 811nm shown in Figure 5. The laser runs at a repetition rate of approximately 90 MHz and is tunable from 800-850 nm. A sample of the mode-locked spectrum can be found in Figure 4. Two TeO₂ AODs (45070-10-10DEG-1.06-X 45070-10-10DEG-1.06-Y) from NEOS Technologies were used to steer the beam. The AOD crystals are driven by a Texas Instruments AD9959 DDS board supplying signals at 50-90 MHz which are amplified to a maximum power of 2 Watts by MiniCircuits ZHL-1-2W RF amplifiers.

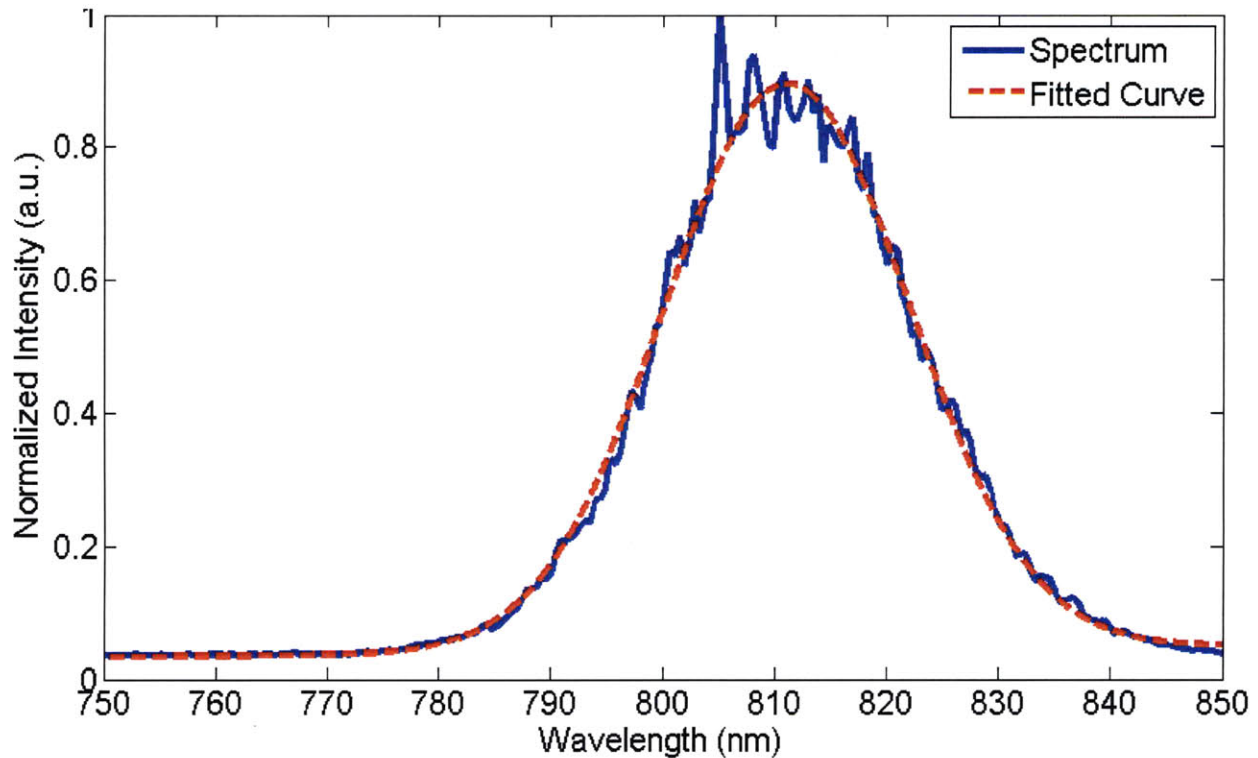


Figure 4: Laser Spectrum. Mode-locked laser spectrum taken with Ocean Optics HR2000 high resolution spectrometer. A Gaussian curve was fit to the spectrum, and the full width at half maximum was 26.7313 nm. The peak wavelength of the fitted curve was 811.1 nm.

Driven at 2 W the AODs have an expected diffraction efficiency of about 20%. Scan lenses were used to relay the AODs to the objective, as well as to expand the beam such that the back aperture of the objective was slightly underfilled. The increased power output of a slightly underfilled objective will be useful for deep tissue imaging and stimulation. At the sample, excitation was at an average power of approximately 2 mW.

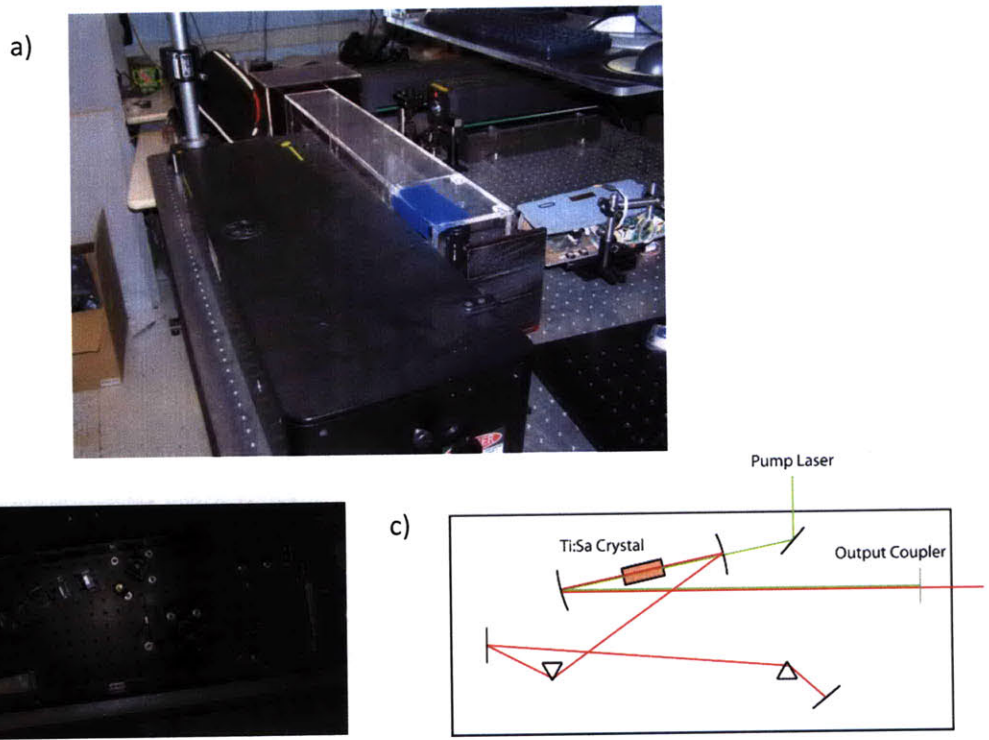


Figure 5: Kapteyn-Murnane Labs Ti:Sa Laser. a) The Ti:Sa crystal is pumped by a 532nm diode laser at 4.75 W. b) A photo of the laser cavity. c) A schematic of the laser cavity. Both prisms and the slight are mounted on stepper motors (not shown) in order to tune and mode-lock the laser.

A Chroma Technology 680 DCSPXR short-pass dichroic filter was used to redirect the excitation laser towards the sample. Extra excitation photons are filtered by a Chroma Technology ETS510/80m-2p bandpass filter. Fluorescence is captured by a H7422P-40 PMT module which sources current to a 10 kOhms terminator. A lens was used to focus fluorescence onto the PMT, and was oversized so as not to limit collection efficiency. The lens is necessary in order to capture as much signal on the PMT as possible, which has a smaller active area than the back aperture of the objective. In addition the lens helps mediate some of the effects of the drop off in collection efficiency that occurs at the edges of the field of view. The efficiency of collection is therefore restricted by the geometry of the objective lens.

The objective used was an Olympus XLUMPFL 20x/0.9 NA objective. The geometry of the objective gives an efficiency of 6% at the focal point. Losses will also occur at the emission filter, collection lens, and dichroic, pushing this efficiency closer to 5%. The objective was chosen because of its high NA and low magnification, which should boost the depth of imaging. The optical path was also extended to allow for future beam shaping equipment and diagnostics, which could boost the power of the laser, or effect the temporal or spatial profiles of the pulses being delivered in order to extend the depth of imaging further. A block schematic of the optical setup can be found in Figure 6.

A LeCroy Waverunner 44xi Oscilloscope reads the signal from the PMTs and controls the TI AD9959 DDS board over USB. The Waverunner Oscilloscope was chosen due to the ruggedized nature of the system, the built in DC-600MHz transimpedance amplifiers, and the speed compared to PC card digitizers. The oscilloscope allowed for an all-in-one solution for control of the DDS board and digitization of the signal.

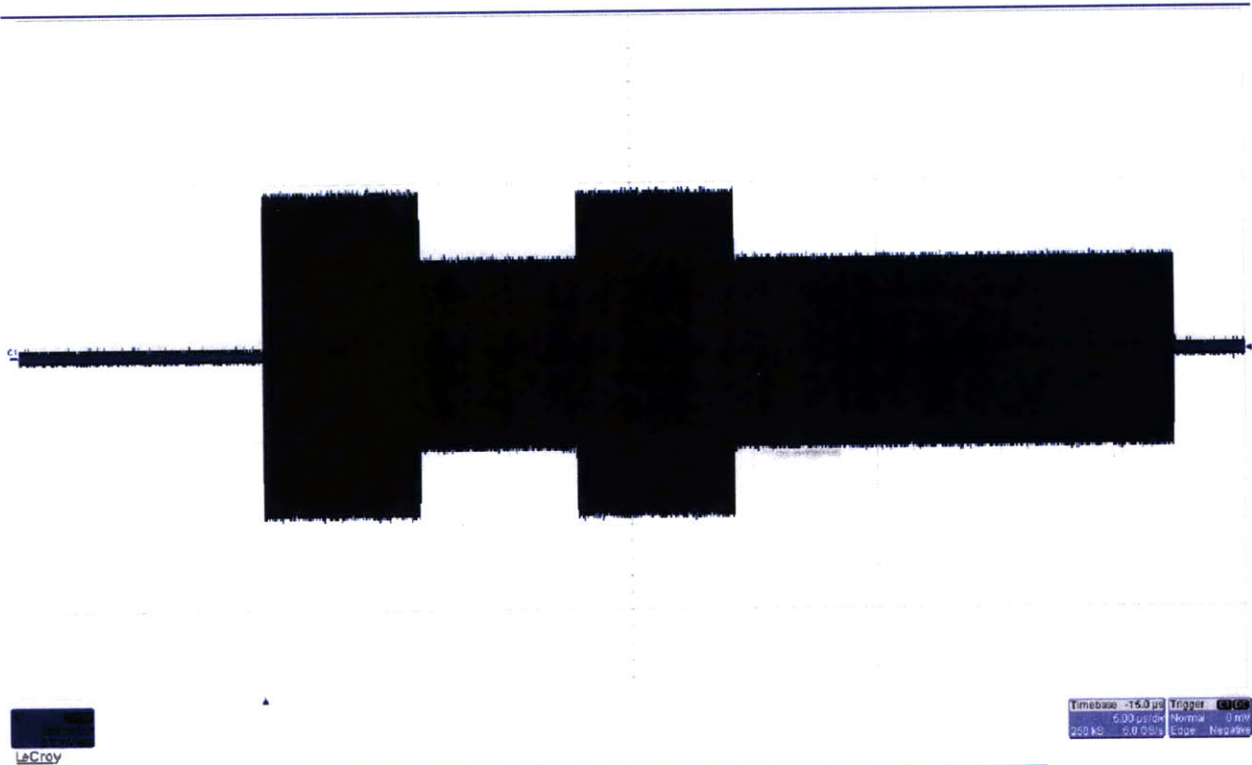
An epifluorescence pathway and an eyepiece were not included since the microscope will be used primarily in vivo. This had the added benefit of lowering the cost of the system and freeing up space around the specimen stage for other necessary equipment. All imaging is done using the PMTs and fluorescence. The field of view is therefore restricted only by the AODs and objective. The maximum field of view for the objective is 1295 μm [10]. Simulations using Code V including the AODs, suggest that the field of view should be approximately 836 μm .

4.2. Neurospy Software

The oscilloscope runs software developed at the Salk Institute for two-photon imaging available for development at www.neurospy.org [15]. The Neurospy software is built on the NetBeans Platform, and is written in Java. It provides an API for the scanner (TI AD9959 DDS), digitizer (Lecroy DSO), and allows for custom microscope configurations. The modular nature of the software makes it ideal for the creation of custom two-photon microscope setups, as it abstracts much of the lower level functions into a user friendly front end for scan development.

The basic imaging protocol samples a frame at 1 MHz and scans 512 lines. At this sampling rate and frame size, imaging should take approximately 262 ms, corresponding to a frame rate of 3.82 frames per second. In actual testing for 100 frames, the average time to scan a single frame was 444.25 ms for a single scan, corresponding to a frame rate of 2.25 frames per second.

Protocols for the random access of points with user specified dwell times and power were written to expand the software for use in photostimulation experiments. The program was developed so that a point could be specified based on the normalized location in a 2D plane. Users are able to specify the points, dwell-time, power, and number of cycles that the scan can will repeat for. Points are given in two Java text fields, corresponding to the x and y location in the 2D plane as a list separated by spaces. Point scanning was improved to 156.25 kHz. A sample waveform for the 2D random access protocol can be found in Figure 7.



LeCroy

Timebase: 15.0 μ s Trigger: 0.00
 0.03 μ s/div Normal 0 nV
 240 kS/s 2.0 0.00s Edge: Negative

b)

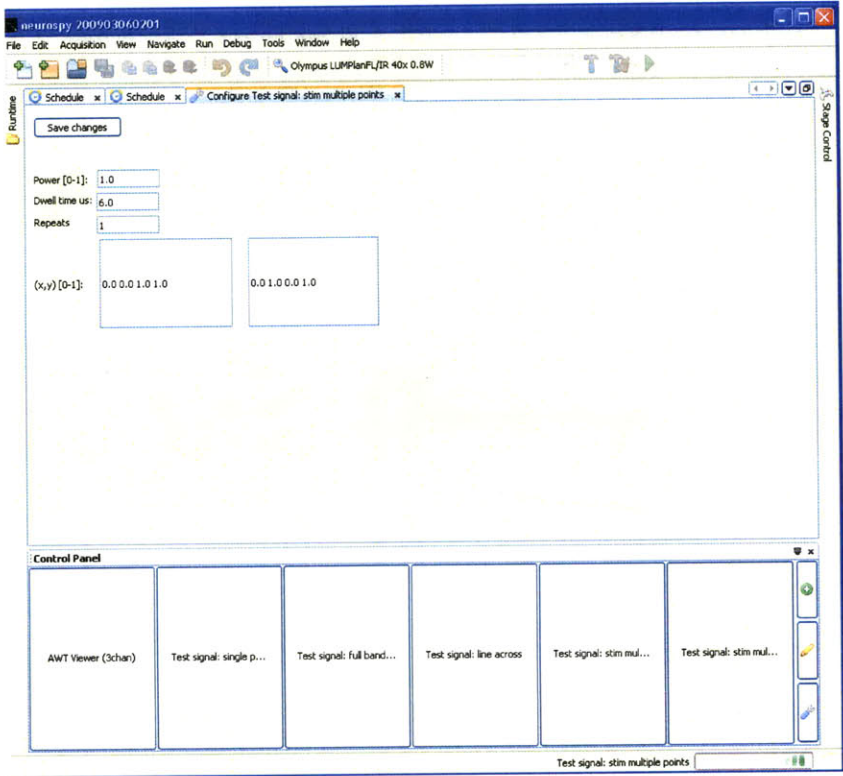


Figure 7: Sample of Random Access Waveform in Two Dimensions. a) Waveform from random access scan for a single channel where the corner of each frame is scanned. The power is at the maximum and the dwell-time at each point is 6 μ s. b) The configuration for the scan shown in a) in the Neurospy software suite.

A 3D scan pattern was also developed in order to allow a user to specify a point in x-y space as well as a chirp duration and length. Current iterations of the scan pattern are limited by the software implementation of single point scanning. Single point rates were approximately 222 kHz. Chirps could be generated for durations as low as 1 μ s, suggesting this limitation is in the software and not the hardware, and thus further improvements can be made. The low scanning speeds are likely the result of the serial nature in which the protocol treats chirps by always returning to the (0,0) point. Scanning could be improved by choosing points in sequence that are close to the end frequency of the prior chirp. A sample of a pulsed waveform generated by the 3D random access protocol can be found in Figure 8. Like the 2D scan pattern, the aim for creating the 3D random access protocol was so that rapid prototyping of scan pattern generation could be developed in parallel. A cell identification algorithm was developed to identify neurons for stimulation which will be outlined further in the Section 5.3.

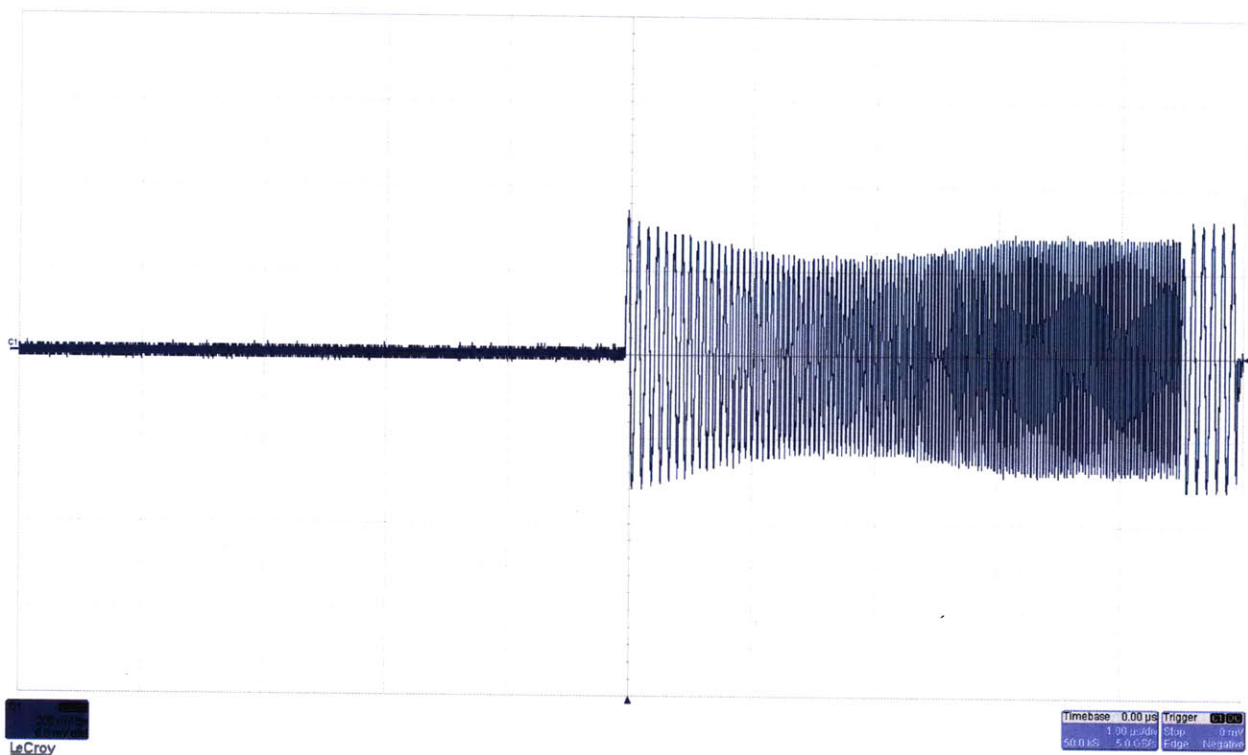


Figure 8: Sample of Chirped Waveform in Three Dimension. A waveform of a chirped pulse on a single channel for random access in three dimensions. The chirp was set for 3 μ s and for the full bandwidth 90-50 MHz.

4.3. Imaging

The first step in imaging was to look at fluorescent wells (fluocells) of fluorescein. This was done in order to characterize the uniformity of illumination of the field of view. Fluocells were constructed using NIST-traceable fluorescein at a nominal concentration of $50\mu\text{M}$ from Invitrogen (F36915). Using a NIST-traceable fluorescein in a self-prepared fluocell has the advantage of being convenient, cheap, and reliable enough to be used for predicting the comparing the actual efficiency to the theoretical efficiency of the microscope. The fluocell minimizes the effects of photobleaching by allowing the fluorescent molecules to move freely. Given a uniform scanned illumination, therefore a uniform fluorescence should be observed.

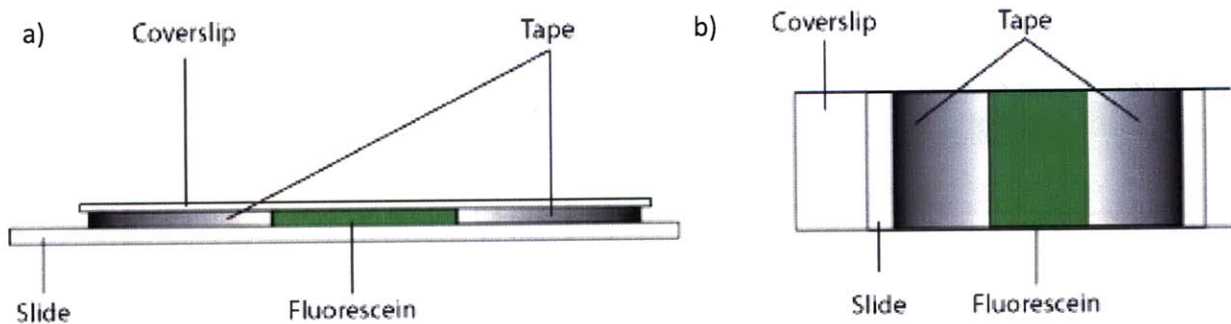


Figure 9: Schematic of Fluorescent Well. A fluocell is a small enclosed well of fluorescent dye. a) Side view of a fluocell. b) Top view of a fluocell.

The next phase of imaging was to look at $1.0\mu\text{m}$ yellow-green fluorescent polystyrene microspheres from Invitrogen (F13081), in order to quantify the resolution and field of view of the microscope. Assuming the brain tissue has an index of refraction close to that of water ($n=1.33$), the Olympus XLUMPFL 20x/0.9 NA objective is used, and excitation is centered at 832 nm , Equation (3.3.1) gives the theoretical limit of resolution in the axial direction as $2.73\mu\text{m}$. In the lateral direction given the same parameters based on Equation (3.3.2) the lateral resolution is 555 nm .

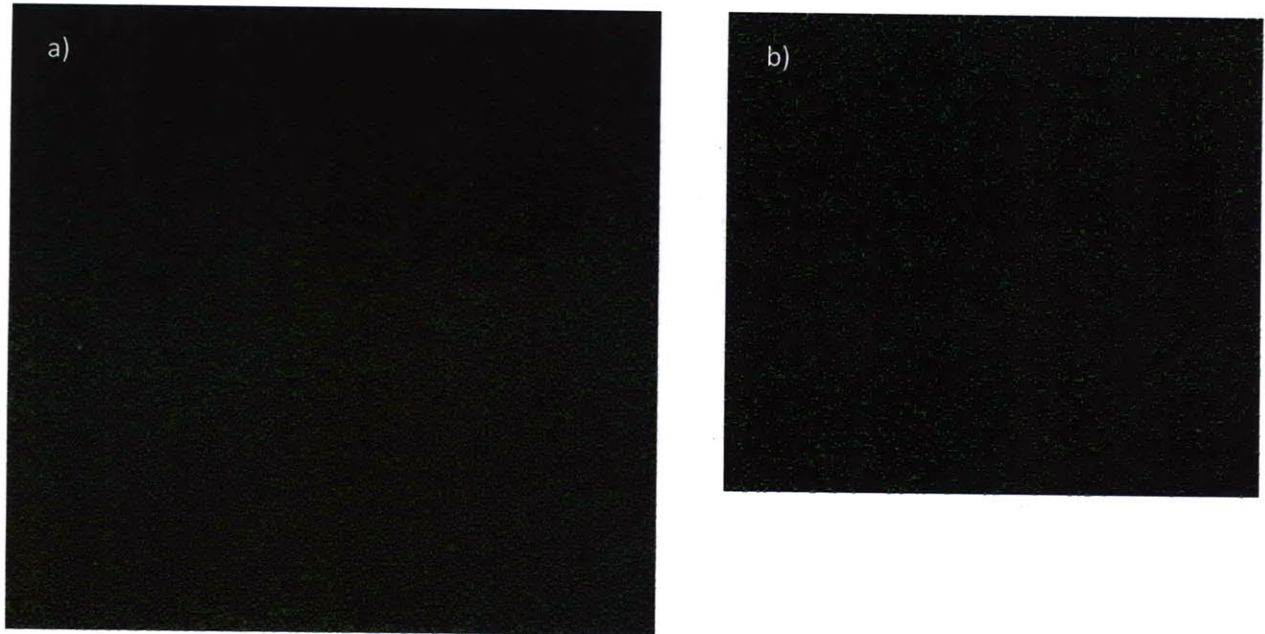


Figure 10: Images of Polystyrene Microsphere. a) $1\mu\text{m}$ yellow-green fluorescent polystyrene microsphere imaged with a confocal microscope at 20x magnification. b) Zoomed in view of lower right corner of a)

A baseline of the noise was taken when imaging a fluocell filled only with water. This noise is from the electrical noise introduced from the PMT and oscilloscope as well as ambient light in the imaging setup. Curtains were used to minimize ambient light, and room lights were turned off for imaging. An image and analysis of the noise can be found in Figure 11. The analysis of the noise suggest that there is periodic noise that degrades the image. Since ambient light is most likely going to contribute random salt and pepper noise to the image, this periodic noise is likely from an electrical source. Minimizing the electrical noise by ensuring all cables are shielded, should improve the overall quality of images. Processing images could also alleviate some of the noise, but could result in the loss of some of useful features of the neurons in the image.

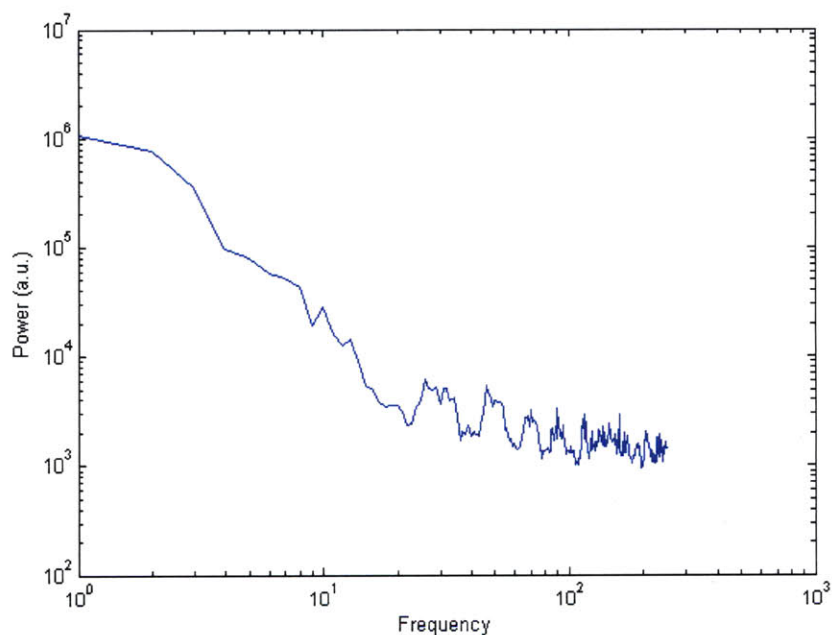


Figure 11: Image and Analysis of Noise. a) Raw image of noise including electrical and ambient light. b) Log-Log plot of the power spectral density of the Image

One problem encountered in imaging was that the power delivered to the sample by the AODs driven by 2W RF and deflecting the 820 nm center wavelength pulsed laser did not appear to be sufficient to get two photon fluorescence at observable levels. While an average of 2 mW at the sample was recorded using a power meter, two-photon excitation of fluorescein was not observed. An IR

viewing card was used to verify that scanning was occurring and can be seen in Figure 12. Since AODs were used, the illumination of the field of view should be fairly even. The field of view for the microscope was not uniformly lit, likely due to variation in the diffraction efficiency of the AODs for different RF frequencies and the geometry at which the AODs were positioned relative to the objective.

At 2 mW excitation for a 820 nm laser the squared average intensity is approximately 9.4×10^{-49} photons² cm⁻⁴ s⁻², assuming a diffraction limited spot of diameter 328 nm. Using a pulsed laser with a repetition rate of ~90 MHz and a Gaussian beam this scales by a factor $\sim 10^5$ to give the average squared intensity of approximately 9.4×10^{-54} photons² cm⁻⁴ s⁻² [16]. The two-photon cross section of fluorescein at 820 nm is 29 GM (cm⁴ s / photon) and the quantum yield is ~.9 [17]. When the pulsed laser is focused to a diffraction limited spot in 50 μM fluorescein, $\sim 1.3 \times 10^9$ photons/s are generated. Given the geometric setup of the microscope, assuming 5% collection efficiency and sampling at 1 MHz, for each pixel 68 photons are collected, corresponding to a current of 4.7 μA sourced by the PMTs . Since the PMTs are current limited to 2 μA this should lead to the PMT saturating causing saturation of the image of the field of view.

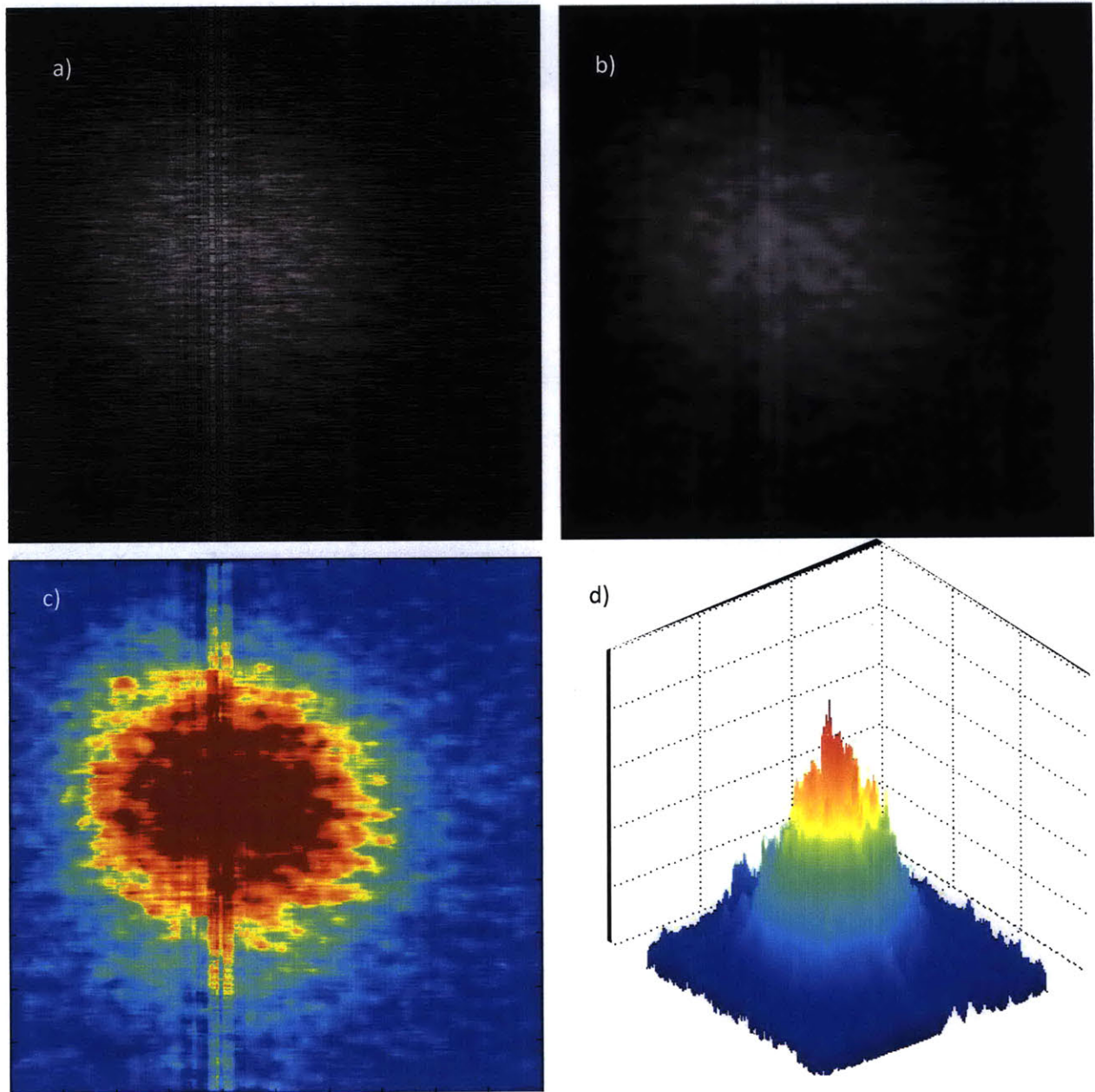


Figure 12: Pattern of Illumination. Infrared viewing card scanned at full bandwidth with AODs. a) Raw image b) Median filtered image with a 10x10 matrix c) Normalized contour map of filtered image d) surface plot of filtered image

Most likely the laser pulse was spatially or temporally broadened, such that a sufficient photon density was not present in the focal volume at the sample to drive two-photon fluorescence at an observable level over the noise. The likely sources of the temporal broadening are the AODs. There are a number of ways which this broadening could be limited. One way is to use four AODs, this however has

the downside of limiting the field of view[18]. Another alternative is to use prism or diffraction gratings to compensate for the temporal broadening before the pulses reach the AODs[19, 20].

Using a GRENOUILLE to view the laser pulses coming out of the AODs would be the first step in diagnosing whether the major culprit is temporal or spatial broadening. If the cause is spatial broadening it is likely due to divergence of the beam before it enters the AODs, and beam sculpting optics would be need to ensure a fully collimated beam is being sent to the AODs. Temporal broadening would require compensation of the pulse shape before the AODs by a method similar to the ones described above.

5. Two-Photon Activation of Targeted ChR2

Within the brain, axons projecting from other brain regions are often densely packed around a particular neuron of interest. The nonspecific expression of ChR2 in dendrites and axons could cause action potentials in colocalized axons of neurons that are not of interest in the neural circuit being mapped. Given their small volume, axons are more likely to trigger action potentials, therefore in order to move towards in vivo mapping of brain circuits, it is necessary to localize the expression of ChR2 to the cell body.

Stimulating a neuron using only the soma, however, can be difficult due to the localized two-photon activation of ChR2, thus it is necessary to have an automated method of identifying ChR2 expressing cells and generating scan patterns. This section will outline the use of Myosin Va binding domain to localize expression of ChR2 to the somatodendritic regions of neurons, and the photostimulation of neurons using two-photon activation of a ChR2-MBD construct expressed in neuron cultures.

5.1. Localization of ChR2

The Myosin Va binding domain has been found to localize expression of ChR2 to the somatodendritic regions of neurons [21]. While the exact mechanism of the Myosin Va is not entirely clear there are two models that could explain how the vesicles with a plus end-directed myosin and kinesin motor interact with cytoskeleton tracks of actin filaments and microtubules to travel to dendrites and not axons. The first is that vesicles propelled by myosin motors travel along actin filaments adjacent to the dendrites. The second is that vesicles are free to attach to any microtubules, but the ones that attach to axonal microtubules are driven towards the plus end which points to the cell

body. The net effect however, is that the movement of these proteins are biased towards the dendrites driving expression of proteins to be contained primarily in the dendrites and soma of the neurons.

By expressing ChR2-MBD in a neuron, the ChR2 protein density in dendrites is more than fivefold higher than in axons, meaning that only the current driven by the focus at the somatodendritic compartments would be sufficient to drive action potentials in neurons. Eliminating the activation of neurons from outside the region of increases the spatial resolution with which a neural circuit can be mapped. The use of genetic expression to do so also opens avenues to target specific cell types in the brain in order to investigate their functions in behaviors and disorders.

A ChR2-MBD construct tagged with GFP was developed by the Synthetic Neurobiology group and was used during experiments. Figure 13 shows confocal images at 20x of the expression of ChR2-MBD (green) compared to tdTomato (red) expressed in the cytosol. Figure 14 shows regular expression of ChR2 for comparison.

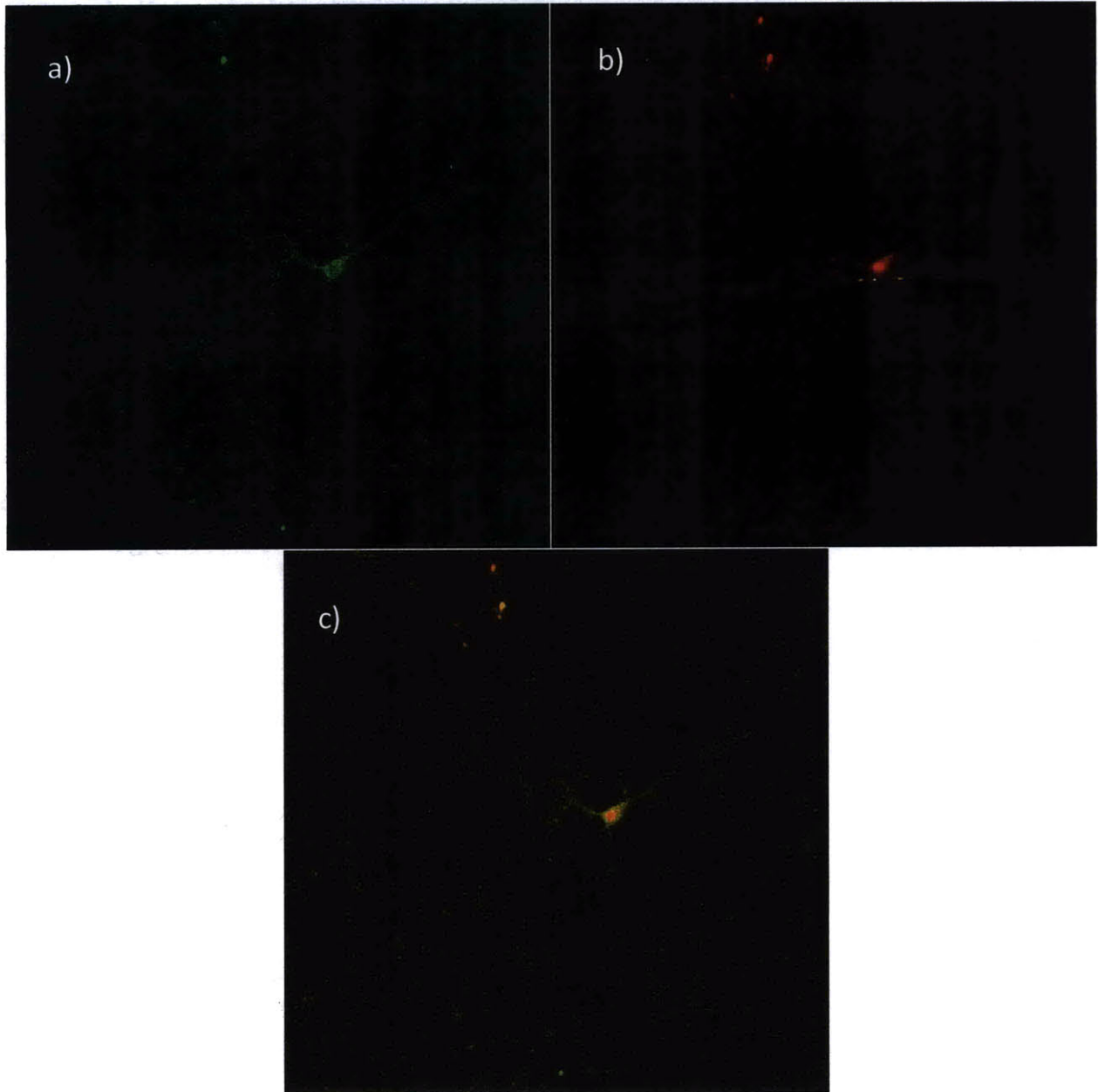


Figure 13: Expression of ChR2-MBD Confocal images of ChR2-MBD-GFP expressing neuron. a) GFP expression b) TdTomato expression in cytosol c) Composite of GFP and tdTomato. Note the GFP expression is primarily confined to the membrane of the cell body.

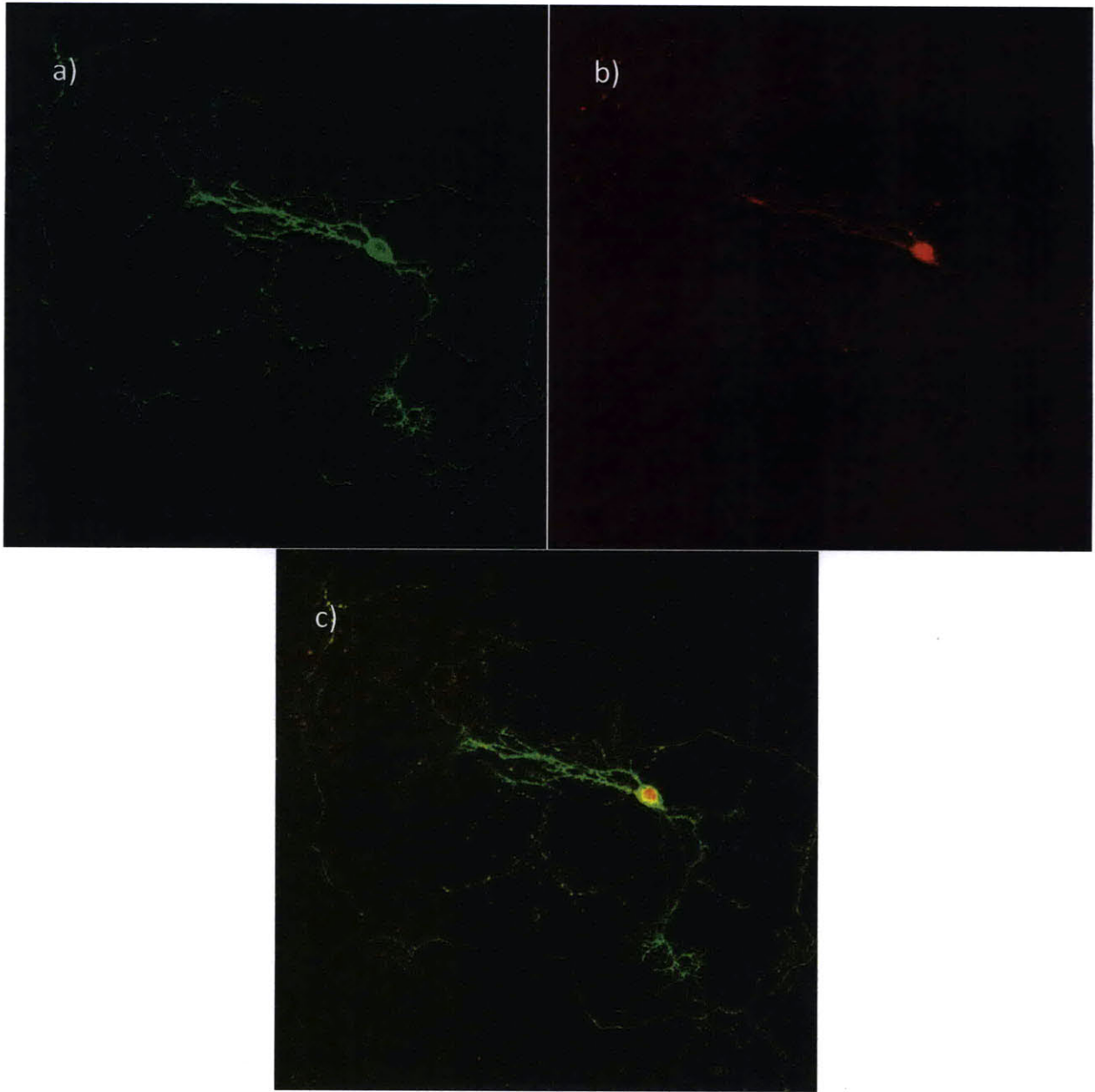


Figure 14: ChR2 expression Confocal images of ChR2-GFP expressing neuron. a) GFP expression b) TdTomato expression in cytosol c) Composite of GFP and tdTomato. Note the GFP expresses throughout the neuron including the axon.

5.2. Two-Photon Activation and Saturation of ChR2

Tank and Rickgauer modeled the saturation limited two-photon activation of ChR2, in order to analyze induced currents across the membrane[6]. Saturation of ChR2 occurs because of the large two-photon cross section and the long lifetime of ChR2 molecules in the conduction state (~10 ms). The model accounts for all ChR2 molecules that undergo at most one photocycle, which contribute to the photocurrent. A brief analysis of the model explains why driving action potentials in a neuron through two-photon stimulation of the soma can be difficult.

When illuminated with light of intensity $I(t)$, concentration of ChR2 molecules in the ground state $\rho_g(t)$ reduces exponentially as:

$$\rho_g(t) = \rho_{g0} e^{-\frac{\sigma_m}{m} I(t)^m t}, \quad (5.2.1.)$$

where σ_m is the multi-photon absorption cross section of the ChR2 molecule (where $m = 1$ for single photon absorption and $m = 2$ for two-photon absorption). In two-dimensions, with radial-symmetric illumination of $I(r, t)^m$ and η is the quantum efficiency the rate of molecules moved to the excited state is modeled by

$$\frac{dN(t)}{dt} = \eta \frac{\sigma_m}{m} \int_S I(r, t)^m \rho_g(r, t) dA \quad (5.2.2.)$$

and the number of molecules in the excited state that contribute to the photocurrent, $N^*(T)$, after a time $t = T$ where $t=0$ is the time of light onset, the ChR2 molecules decay from the excited state at the rate τ_2 and τ_1 is the latency of excitation, is given by the equation

$$N^*(T) = \int_0^T \frac{dN(t)}{dt} \left[e^{-\frac{T-t}{\tau_2}} - e^{-\frac{T-t}{\tau_1}} \right] dt. \quad (5.2.3.)$$

Thus Tank and Rickgauer derived the fraction of available photocurrent (the instantaneous photo current $I^*(T)$ over the total available photo current I_{max}^*),

$$\frac{I^*(T)}{I_{max}^*} = \frac{N^*(T)}{\eta N_t}. \quad (5.2.4.)$$

in a population of N_t molecules[6].

There are two approaches to inducing photocurrents in neurons. A graphical comparison of the two methods can be found in Figure 15. The first approach to photo-stimulating the cell is to diffusely focused a pulsed laser over the entire cell. ChR2 excitation occurs throughout the entire neuron. The downside is that it requires high powers in order to get the activation, since the neuron is outside of the focal volume. This approach is therefore not as useful for in vivo applications since the high powers could damage tissue, or activation of ChR2 in neurons above or below the neuron of interest.

Another approach is to induce photocurrents primarily at the focal point, by using a lower power. In this regime, Tank and Rickgauer solved for the fraction of available photo current, for a

uniform concentration of molecules and a scan at a constant velocity such that molecules are excited at a constant rate. The solution to equation (5.2.4) is approximated by the equation

$$\frac{I^*(T)}{I_{max}^*} = \frac{\tau_2}{T_s} \left(1 - e^{-\frac{T_s}{\tau_2}}\right) \quad (5.2.5.)$$

where T_s is the total scan time and $T_s > \tau_1$ [6]. Since the peak current scales inversely with T_s it would suggest that a faster scan is most desirable when trying depolarize the neuron. This approach requires fast scanning, but has the added benefit of being useful in deep tissue where laser powers may be low.

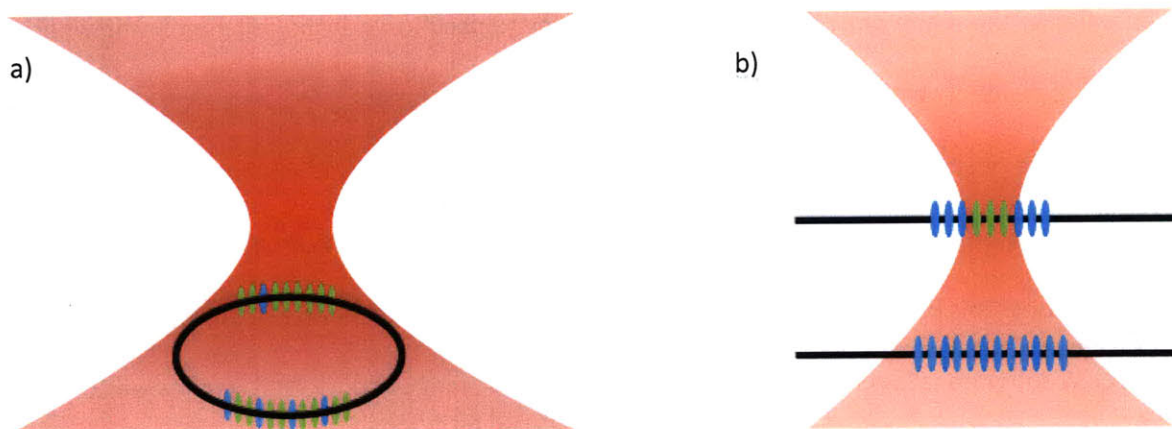


Figure 15: Two-Photon Activation of ChR2 a) Whole cell stimulation of ChR2 is achievable with a high power, diffuse illumination of the cell. Excitation of ChR2 (green ellipses) is spread throughout the membrane. b) Excitation of ChR2 can occur only at the focal region of the laser at a lower power.

5.3. Scanning ChR2

Rickgauer and Tank used galvanometer based mirrors to scan in a spiral pattern in a cell and a mechanical iris to extend the beam waist along the optical axis [6]. By employing the AOD scanner, scanning in three dimensions can be sped up. Since the focal spot is moving when the AODs are

scanning in 3D an optimal scan pattern can be found. A Matlab script was tested that could take user identified neurons, based on mouse clicks, and give a series of points on concentric ellipses. As a basis for testing, the pattern was only developed for a single image in a single plane. Since chirp rates were not calculated based on the image, the assumption was made that the cell is approximately a spheroid and the user would define the appropriate chirp rate for each point or ellipse. A sample of a scan pattern that was generated is shown in Figure 16. Automation of analysis however, has many desirable advantages including standardization of image acquisition parameters and higher throughput [22].

Currently an algorithm that can skeletonize a neuron for the identification in three dimensions is in development. By taking a stack of images a scan patterns in three dimensions could be generated that can approximate the shape of a neuron, allowing scanning to occur only at the cell membrane where the ChR2 proteins reside. With fast scanning and good scan patterns the goal is to drive high enough currents to cause neurons to action potential even at the lower laser powers encountered in deep tissue. The Neurospy software was thus expanded to take lists of points in normalized coordinates in 2 and 3 dimensions. This design was chosen so that image analysis could be developed separately from the Neurospy software, allowing for the rapid development of image analysis software as was outlined in Section 4.2.

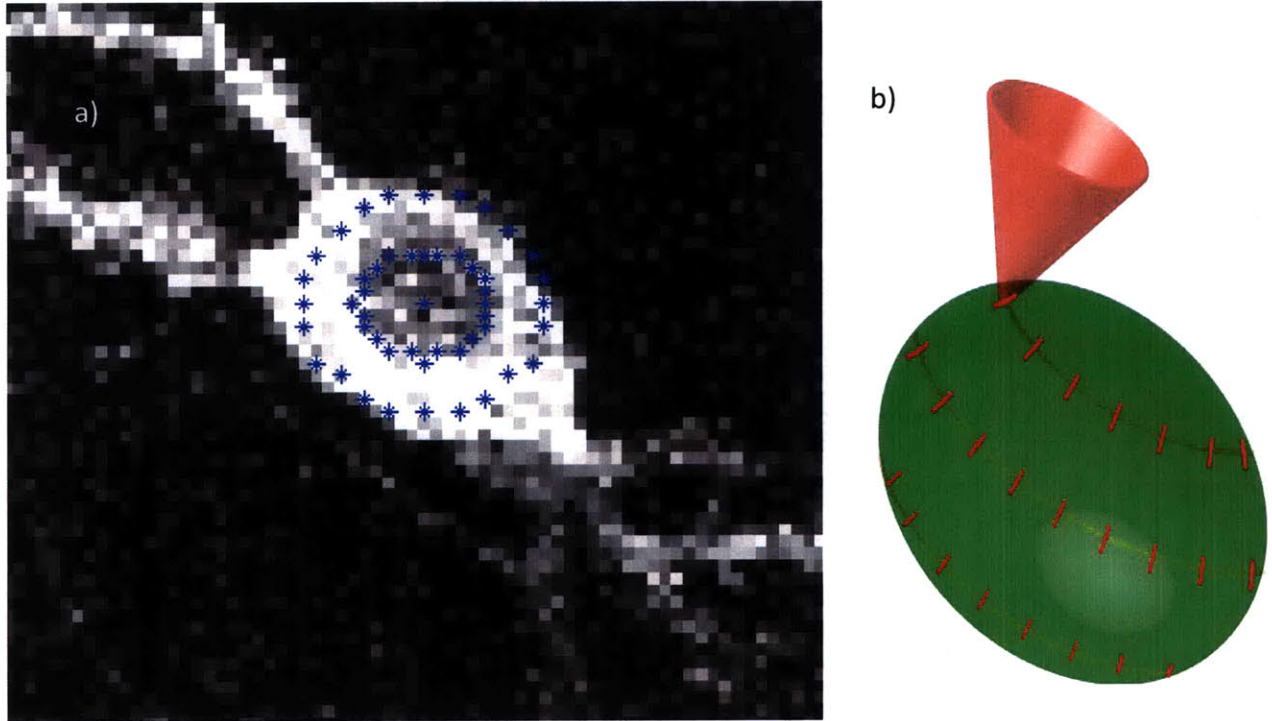


Figure 16: Generated Scan Pattern. a) Sample scan pattern generated by Matlab script from a user identified cell. Since scan pattern is based on a 2D image chirp rates must be defined by the user. b) Schematic of scan pattern assuming the cell is a spheroid and a constant chirp rate is chosen for each ellipse generated the Matlab script

6. Further Work

This thesis has outlined the technology needed to image and stimulate a neuron using two-photon activation of ChR2. The two-photon microscope must still be tested to determine the cause of the low power output that is preventing two-photon absorption, and proper optics must be put in place that will prevent either the temporal or spatial broadening and allow for deep tissue imaging. In addition in order to move towards imaging and stimulation in deep tissue, increasing the efficiency of the AODs by driving that at higher powers would help to increase the power available at the focal point.

Beyond imaging, the next step is to test activation using patch-clamping of stimulated neurons in slices of brain tissue and neurons downstream. Patch clamping will allow scan patterns to be optimized in order to get reliable stimulation of action potentials in neurons. To demonstrate the consistency of the optical stimulation and compare it to traditional electrode stimulation it will be necessary to test the effects of stimulation in a well known paradigm. Long term potentiation (LTP) in the hippocampus is fairly well understood and can be induced using electrodes in slices [23, 24]. Reproducing LTP in hippocampal slices would go towards validating two-photon activation of ChR2 as a method for stimulating neurons in a specific manner for mapping of neural circuits.

To move towards work that is carried out completely in vivo, it is necessary to minimize or reduce all use of electrodes. Patch clamping allows the electrical signals within neurons to be recorded, but still requires the physical insertion of an electrode into the brain. Voltage sensitive fluorescent proteins (VSFPs) provide an option for completely optical readout. These fluorescent proteins can be expressed in the membrane of a neuron, and are reactive to voltage changes across the membrane using conformational changes that effect Förster resonance energy transfer or intrinsic fluorescence [25-

27]. Many of these proteins can add parasitic capacitance to the neuron, however, altering the electrical properties of the neuron [28]. Much work is still required in this area to develop better VSFPs , but using two-photon activation of both ChR2 and a suitable VSFP could allow for long-term mapping of neural circuits in vivo.

7. Conclusions

Fast scanning two-photon microscopy coupled with the use of light activated ion channels provides the basis for fast imaging and stimulation in the characterization of in vivo neural networks. This thesis developed some of the building blocks needed to have a system for in vivo imaging and stimulation of neurons. The first stage was the design and construction of a two-photon microscope capable of fast scanning using acousto-optic deflectors. While the optical power was insufficient to gather images using two-photon absorption, only minor modifications are necessary to move toward that goal.

The second stage was to develop software that can identify neurons from images acquired using the two-photon microscope and generate scan patterns in three dimensions. Here the software controls for the microscope were expanded such that 2D scans could be developed in a modular way. The software was also expanded so that lists of points in 3 dimensions could also be accepted, paving the way for scan patterns that can be tailored to the shape of individual cells targeting the cell membrane where the optogenetic protein ChR2 resides.

The final stage concerns localization of the optogenetic channelrhodopsin-2 channel at the neuron cell body. The necessity for fast scanning and the localization of ChR2 to the soma was discussed. The use of a fast scanning acousto-optic two-photon microscope with software that can identify and customize scans to individual cells should allow for high enough currents for action potentials to occur in neurons even at low laser powers.

8. References

1. Boyden, E.S., et al., *Millisecond-timescale, genetically targeted optical control of neural activity*. Nat Neurosci, 2005. **8**(9): p. 1263-8.
2. Gradinaru, V., et al., *Optical deconstruction of parkinsonian neural circuitry*. Science, 2009. **324**(5925): p. 354-9.
3. Wyart, C., et al., *Optogenetic dissection of a behavioural module in the vertebrate spinal cord*. Nature, 2009. **461**(7262): p. 407-10.
4. Tsai, P., et al., *Principles, Design, and Construction of a Two-Photon Laser-Scanning Microscope for In Vitro and In Vivo Brain Imaging*, in *In Vivo Optical Imaging of Brain Function*. 2009, CRC Press.
5. Mohanty, S.K., et al., *In-depth activation of channelrhodopsin 2-sensitized excitable cells with high spatial resolution using two-photon excitation with a near-infrared laser microbeam*. Biophys J, 2008. **95**(8): p. 3916-26.
6. Rickgauer, J.P. and D.W. Tank, *Two-photon excitation of channelrhodopsin-2 at saturation*. Proc Natl Acad Sci U S A, 2009. **106**(35): p. 15025-30.
7. Denk, W., J.H. Strickler, and W.W. Webb, *Two-photon laser scanning fluorescence microscopy*. Science, 1990. **248**(4951): p. 73-76.
8. Denk, W. and K. Svoboda, *Photon upmanship: why multiphoton imaging is more than a gimmick*. Neuron, 1997. **18**(3): p. 351-7.
9. So, P.T.C., et al., *TWO-PHOTON EXCITATION FLUORESCENCE MICROSCOPY*. Annual Review of Biomedical Engineering, 2000. **2**(1): p. 399-429.
10. Oheim, M., et al., *Two-photon microscopy in brain tissue: parameters influencing the imaging depth*. Journal of Neuroscience Methods, 2001. **111**(1): p. 29-37.
11. Levene, M.J., et al., *In Vivo Multiphoton Microscopy of Deep Brain Tissue*. J Neurophysiol, 2004. **91**(4): p. 1908-1912.
12. Theer, P. and W. Denk, *On the fundamental imaging-depth limit in two-photon microscopy*. J. Opt. Soc. Am. A, 2006. **23**(12): p. 3139-3149.
13. Reddy, G.D. and P. Saggau, *Fast three-dimensional laser scanning scheme using acousto-optic deflectors*. J Biomed Opt, 2005. **10**(6): p. 064038.
14. Duemani Reddy, G., et al., *Three-dimensional random access multiphoton microscopy for functional imaging of neuronal activity*. Nat Neurosci, 2008. **11**(6): p. 713-720.
15. Vucinic, D. and T.J. Sejnowski, *A compact multiphoton 3D imaging system for recording fast neuronal activity*. PLoS ONE, 2007. **2**(1): p. e699.
16. Zipfel, W.R., R.M. Williams, and W.W. Webb, *Nonlinear magic: multiphoton microscopy in the biosciences*. Nat Biotech, 2003. **21**(11): p. 1369-1377.
17. Albota, M.A., C. Xu, and W.W. Webb, *Two-Photon Fluorescence Excitation Cross Sections of Biomolecular Probes from 690 to 960 nm*. Appl. Opt., 1998. **37**(31): p. 7352-7356.
18. Kremer, Y., et al., *A spatio-temporally compensated acousto-optic scanner for two-photon microscopy providing large field of view*. Opt. Express, 2008. **16**(14): p. 10066-10076.
19. Pessot, M., P. Maine, and G. Mourou, *1000 times expansion/compression of optical pulses for chirped pulse amplification*. Optics Communications, 1987. **62**(6): p. 419-421.
20. Bor, Z. and B. Rácz, *Group velocity dispersion in prisms and its application to pulse compression and travelling-wave excitation*. Optics Communications, 1985. **54**(3): p. 165-170.
21. Lewis, T.L., et al., *Myosin-dependent targeting of transmembrane proteins to neuronal dendrites*. Nat Neurosci, 2009. **12**(5): p. 568-576.

22. Dragunow, M., *High-content analysis in neuroscience*. Nat Rev Neurosci, 2008. **9**(10): p. 779-788.
23. Malenka, R.C., *Synaptic plasticity in the hippocampus: LTP and LTD*. Cell, 1994. **78**(4): p. 535-538.
24. Whitlock, J.R., et al., *Learning Induces Long-Term Potentiation in the Hippocampus*. Science, 2006. **313**(5790): p. 1093-1097.
25. Perron, A., et al., *Second and third generation voltage-sensitive fluorescent proteins for monitoring membrane potential*. Front Mol Neurosci, 2009. **2**: p. 5.
26. Tsutsui, H., et al., *Improving membrane voltage measurements using FRET with new fluorescent proteins*. Nat Meth, 2008. **5**(8): p. 683-685.
27. Villalba-Galea, C.A., et al., *Charge Movement of a Voltage-Sensitive Fluorescent Protein*. Biophysical Journal, 2009. **96**(2): p. L19-L21.
28. Akemann, W., et al., *Effect of Voltage Sensitive Fluorescent Proteins on Neuronal Excitability*. Biophysical Journal, 2009. **96**(10): p. 3959-3976.